AIAA Meeting Papers on Disc, January 1996
A9618860, NSF CTS-90-19813, NSF CTS-93-21959, AIAA Paper 96-0912

Markstein numbers and unstretched laminar burning velocities of wet carbon monoxide flames

M. I. Hassan
Michigan Univ., Ann Arbor

K. T. Aung
Michigan Univ., Ann Arbor

G. M. Faeth
Michigan Univ., Ann Arbor

AIAA 34th Aerospace Sciences Meeting and Exhibit, Reno, NV Jan 15-18, 1996

Effects of positive flame stretch on the laminar burning velocities of wet carbon monoxide/air flames at normal temperature and pressure were studied both experimentally and computationally. Measurements and numerical simulations considered outwardly-propagating spherical laminar premixed flames having both stable and unstable preferential diffusion behavior. Test conditions included concentrations of hydrogen in the fuel mixture of 3-50 percent by volume, fuel equivalence ratios of 0.6-5.0, Karlovitz numbers of 0-0.91, and laminar burning velocities corrected to unstretched (plane) flame conditions of 130-1730 mm/s. Both measured and predicted ratios of unstretched to stretched laminar burning velocities varied linearly with Karlovitz numbers, yielding Markstein numbers in the range -6.5 to 7.6, reaching largest values near limits for the largest hydrogen concentrations in the fuel mixture. Effects of stretch on luminar burning velocities were modest at low hydrogen concentrations but approached earlier observations for hydrogen/air flames as hydrogen concentrations increased. (Author)

MARKSTEIN NUMBERS AND UNSTRETCHED LAMINAR BURNING VELOCITIES OF WET CARBON MONOXIDE FLAMES

M. I. Hassan,* K. T. Aung† and G. M. Faeth**
Department of Aerospace Engineering
The University of Michigan
Ann Arbor, Michigan 48109-2118

Abstract

Effects of positive flame stretch on the laminar burning velocities of wet carbon-monoxide/air flames at normal temperature and pressure were studied both experimentally and computationally. Measurements and numerical simulations considered outwardly-propagating spherical laminar premixed flames having both stable and unstable preferential-diffusion behavior. Test conditions included concentrations of hydrogen in the fuel mixture of 3-50% by volume, fuel equivalence ratios of 0.6-5.0, Karlovitz numbers of 0-0.91 and laminar burning velocities corrected to unstretched (plane) flame conditions of 130-1730 mm/s. Both measured and predicted ratios of unstretched (plane) to stretched laminar burning velocities varied linearly with Karlovitz numbers, yielding Markstein numbers in the range -6.5 to 7.6, reaching largest values near limits for the largest hydrogen concentrations in the fuel mixture. Effects of stretch on laminar burning velocities were modest at low hydrogen concentrations but approached earlier observations for hydrogen/air flames as hydrogen concentrations increased. Present and earlier stretch-corrected measurements of the laminar burning velocities and Markstein numbers for unstretched (plane) flames were generally in good agreement, aside from some exceptions at conditions where Markstein numbers were large. Predicted and measured unstretched laminar burning velocities and Markstein numbers were in fair agreement, using a chemical reaction mechanism due to Kim et al. (1994); nevertheless, additional development of the mechanism is needed to improve predictions of Markstein numbers over the test range, and unstretched laminar burning velocities at large hydrogen concentrations and fuel-equivalence ratios.

Nomenclature

D	mass diffusivity
K	flame stretch
Ka	Karlovitz number, $KD_{\mathcal{D}}/S_L^2$
L	Markstein length, Eq. (1)
Ma	Markstein number, L/δ_D
Q	chemical energy release per unit mass of reactants
r_f	flame radius
S_L	laminar burning velocity based on unburned gas properties
t	time
T	temperature
δ_D	characteristic flame thickness, $D_{\mathcal{D}}/S_L$
ρ	density
ϕ	fuel-equivalence ratio
Subscripts	
b	burned gas properties
max	maximum observed value
u	unburned gas properties
∞	asymptotic condition for an unstretched (plane) flame

Introduction

Recent experimental and computational studies of effects of flame stretch on laminar premixed flames involving hydrogen/ oxygen/nitrogen and hydrocarbon/air mixtures (H/O/N mixtures) in this laboratory,[1-4] were extended to consider wet carbon-monoxide/air flames (C/H/O/N mixtures) at normal temperature and pressure (NTP). The study involved experimental observations of outwardly-propagating spherical flames in order to find laminar burning velocities as a function of flame stretch (represented by the Karlovitz number), the sensitivity of laminar burning velocities to flame stretch (represented by the Markstein number), and the fundamental laminar burning velocities of unstretched (plane) flames. In addition, the measurements were used to evaluate a recently proposed C/H/O chemical reaction rate

*Visiting Scholar from Helwan University, Cairo, Egypt.
†Graduate Student Research Assistant.
**Professor, Fellow AIAA.

mechanism due to Yetter and coworkers,[5,6] based on corresponding numerical simulations of outwardly-propagating spherical flames that were analyzed in the same manner as the measurements.

Aspects of the interactions between flame stretch and the structure, stability and speed of laminar premixed flames are discussed in several review articles.[7-10] An important finding of recent studies is that interactions between the preferential diffusion of heat and various species, and flame stretch, are unusually significant,[1-4,7-19] which affects the rate of distortion of flame surfaces by turbulence, and thus the propagation of turbulent flames, even in strongly turbulent environments.[1] These results also suggest that past measurements of laminar burning velocities, which are important for understanding and modeling flame properties, should be assessed for effects of stretch that are invariably present when these properties are measured. Finally, the sensitivity of premixed laminar flames to stretch, which is conveniently represented by the Markstein number, provides a new flame parameter that is potentially useful for understanding the propagation and stability properties of laminar premixed flames and for evaluating the performance of detailed numerical simulations of their structure. Thus, there is ample motivation to study the preferential diffusion/stretch interactions of laminar premixed flames at the present time.

The experiments reported here involved observations of outwardly-propagating spherical flames for conditions where $\delta_D/r_f << 1$ and effects of ignition disturbances and radiative heat losses were small. For such conditions, effects of finite flame thickness, curvature and unsteadiness are small,[2] and the relationship between the laminar burning velocity and flame stretch can be represented conveniently by combining an early proposal of Markstein[20] with the "local conditions" hypothesis of Kwon et al.,[1] to yield the following expression:

$$S_{L,o}/S_L = 1 + MaKa \qquad (1)$$

where the dimensionless Karlovitz and Markstein numbers characterize flame stretch, and the response of the flame to stretch, as follows:

$$Ka = K\delta_D/S_L, \quad Ma = L/\delta_D \qquad (2)$$

while δ_D is based on the laminar burning velocity and the mass diffusivity of the fuel in the unburned gas (by convention), as follows:

$$\delta_D = D_u/S_L \qquad (3)$$

Several other proposals have been made to represent effects of flame stretch on laminar burning velocities, see Refs. 7, 8 and 15-19; nevertheless, Eqs. (1)-(3) are particularly convenient because Ma has proven to be relatively constant for wide ranges of Ka. Thus, $S_{L,o}$ and Ma provide concise measures of flame properties that will be used to summarize the experimental and computa-tional findings of the present investigation.

The properties of the laminar burning velocities of wet carbon-monoxide/air flames at NTP were considered during several previous experimental investigations, see Refs. 17, 21-27, and references cited therein. McLean et al.[17] studied outwardly-propagating spherical flames similar to the present investigation, while using a different extrapolation procedure to estimate unstretched laminar burning velocities for hydrogen concentrations of 5 and 50% by volume in the fuel mixture, however, the response of these flames to stretch was not quantified. Vagelopoulos and Egolfopoulos[21] measured laminar burning velocities using the counterflow twin-flame technique (with an empirical extrapolation procedure to estimate unstretched laminar burning velocities) and extinction strain rates; however, these results were limited to lean flames and similar to Ref. 17, flame response to stretch was not quantified. Earlier studies of laminar burning velocities, such as Refs. 22-27 and references cited therein, did not consider effects of stretch and yielded laminar burning velocities that differed from stretch-corrected results as discussed by McLean et al.[17]

Due to the importance of C/H/O chemistry for most practical combustion processes, detailed numerical simulations of wet carbon-monoxide/air flames, and other reaction processes involving carbon monoxide in the presence of hydrogen, have received considerable attention. Past studies include the extensive work of Dixon-Lewis and coworkers,[10,28] McLean et al.[17] and Olsson and Olsson[29] for laminar premixed wet carbon-monoxide/air flames as well as simulations of flow reactor processes due to Kim et al.[5] Similar to past experimental work concerning wet carbon-monoxide/air flames, however, these studies did not address flame response to stretch.

Review of past work suggests that new measurements and computations of the properties of wet carbon-monoxide/air flames at NTP are needed, emphasizing stretch-corrected laminar burning velocities, in order to check past work and expand the range of reactant mixtures considered, and the response

of these flames to stretch. Thus, the present investigation had the following objectives: (1) to measure the properties of outwardly-propagating spherical flames of wet carbon-monoxide/air mixtures at NTP, (2) to complete corresponding numerical simulations of the test flames, (3) to reduce both the measurements and the numerical simulations to find characteristic laminar flame properties ($S_{L,}$ and Ma), (4) to compare the measurements and predictions with each other and with earlier results in the literature, and (5) to exploit the predictions of flame structure to gain insight about prefer-ential-diffusion/flame-stretch interactions. Present measurements were limited to conditions where $\delta_D/r_f << 1$ and radiative heat losses were small, in order to avoid problems of treating flame unsteadiness, curvature and radiative transport; therefore, behavior near flammability limits, quenching conditions and at very small hydrogen concentrations could not be assessed. The chemical reaction mechanism considered during the numerical simulations was limited to the recent results of Yetter and coworkers,[5,6] which is typical of methods used in the literature.

The present discussion begins with descriptions of experimental and computational methods. Results are then considered, treating flame stability and evolution, burning-velocity/stretch interac-tions, Markstein numbers, unstretched laminar burning velocities, sensitivity analysis of the chemical reaction mechanism and flame-structure/stretch interactions, in turn.

Experimental Methods

Apparatus

The present experimental methods were similar to Ref. 4. The measurements were carried out in a spherical chamber having a volume of 0.024 m^3 with an inside diameter of 360 mm. Optical access was provided by two 100 mm diameter quartz windows mounted opposite one another. The chamber was capable of operation over a pressure range extending from complete vacuum up to a maximum of 3.4 Mpa.

The reactant mixture was prepared within a separate chamber by adding gases, at appropriate partial pressures, and then supplied to the test chamber to reach an initial pressure of 1 atm for all tests reported here. All motion of the test gases was allowed to decay so that the gas was motionless when ignited. After combustion was complete, the chamber was vented to the laboratory exhaust system and then purged with dry air to remove residual products prior to refilling for the next test.

The combustible mixture was spark-ignited at the center of the chamber using electrodes extending across the chamber at a 45° angle from the horizontal. One electrode was fixed while the other could be moved with a micrometer having a positioning accuracy of 10 μm. The tips of the electrodes were fine wires (tungsten wire having a diameter of 250 μm and a free length of 40 mm), with a spark gap varying from 1.5-2.5 mm (with larger gaps used to ignite flames near limits where ignition energies become large). The spark energy was supplied by a high-voltage capacitor discharge circuit having a variable capacitance (100-7000 pF) and voltage (0-15 kV), and a discharge time of roughly 5 μs. Spark energies were adjusted by trial so that they were close to the minimum ignition energy (5-20 mJ, with the larger values used near limits, as noted earlier), in order to minimize effects of initial flame acceleration due to excessive spark energies.

Instrumentation

Measurements involved observing the flames using shadowgraph motion picture photography. The shadowgraph system was based on a 100 W mercury short arc lamp (ARC, HSA-150 HP), with the light collimated by a pair of f6 parabolic reflectors having focal lengths of 1220 mm. The flame images were recorded using a 16 mm motion picture camera (Hycam, Model K20 S45) operating at speeds up to 6000 pictures per second to yield exposure times as short as 16 μs. Kodak Plus X and Tri X film were used for the photographs, depending on the camera speed. The framing rate of the camera was sensed electronically so that ignition only occurred when the proper framing rate was reached. The framing rate and the ignition pulse were recorded using a digital oscilloscope (LeCroy 9400A) so that film records could be synchronized.

The film records were measured by projecting them using an Athena Model 224 (MK VIII) projector with an overall magnification of the projected images of 4:1. The flames were nearly spherical (maximum and minimum diameters were within 10% of the mean diameter) but were measured normal to the electrodes to avoid the disturbances due to their presence. The resolution of the flame diameter measurements generally was better than 150 μm.

Data Reduction

Measurements of laminar burning velocities were limited to relatively small flames having diameters less than 60 mm. For such conditions, the volume of burned gas was less than 0.5% of the total chamber volume so that the chamber pressure was constant within 0.7%. Earlier laser velocimeter measurements indicated that velocities within the unburned gas corresponded to behavior expected for unconfined freely propagating spherical flames;[1] therefore, it was assumed that effects of motion in the burned gas, and flow disturbances due to the presence of the chamber walls, were small.

Present measurements were limited to conditions where $\delta_D/r_f \leq 0.02$ which implies negligible curvature and transient effects associated with the thickness of flame, as discussed by Tseng et al.[2] (As noted in Ref. 2, however, present results formally correspond to use of the hot flame boundary reference frame, defined by Clavin.[7]) In addition, rates of radiative heat loss were less than 5% of the rate of chemical energy release within the test flames, based on computations assuming adiabatic flame conditions throughout the burned gas region, and carried out as discussed by Siegal and Howell.[30] Finally, effects of energy release due to ignition were small (less than 20 times the energy release due to combustion) for conditions used to find flame properties. For these conditions, Strehlow and Savage[31] show that the laminar burning velocity is given by the following quasi-steady expression:

$$S_L = (\rho_b/\rho_u)dr_f/dt \qquad (4)$$

with a corresponding expression for K as follows:

$$K = (2/r_f)\, dr_f/dt \qquad (5)$$

Following past practice,[1-4] S_L was found from Eq (4) assuming adiabatic combustion at constant pressure with the reactant temperature equal to the initial temperature and with the same fuel-equivalence ratio in the unburned and burned gases. Then, the density ratio needed in Eq (4) was found by assuming thermodynamic equilibrium in the combustion products for adiabatic, constant pressure and constant fuel-equivalence ratio combustion, using the CEC algorithm of Gordon and McBride.[32] It should be noted, however, that this is a convention that ignores preferential-diffusion effects that modify the local mixture fraction and thermal energy transport for stretched flames and thus the local density ratio ρ_b/ρ_u across the flames. This convention is convenient because a single density ratio is used to relate flame speeds and laminar burning velocities for all levels of flame stretch, which avoids current uncertainties about the effects of stretch on the jump conditions across flames for particular conditions in the unburned gas. Nevertheless, it should be recognized that the density ratio computed in the present manner only is appropriate for an unstretched (plane) flame.

Experimental uncertainties (95% confidence) of dr_f/dt and S_L were less than 5 and 10%, respectively. The higher uncertainty of S_L reflects estimated uncertainties in the basic density ratio of Eq. (4) due to radiative heat losses, approach to equilibrium and potential effects of the slight chamber pressure increase, as well as effects of unsteadiness and radiative heat losses in the burned gas as discussed by Lewis and von Elbe.[33] The corresponding uncertainties of Ka from Eqs. (2) and (5) generally were less than 21%.

Test Conditions

Present test conditions and major results (ρ_u/ρ_b, $S_{L,u}$, Ka_{max} and Ma) are summarized in Table 1. The test range includes concentrations of hydrogen in the fuel mixture of 3-50% by volume, fuel-equivalence ratios of 0.6-5.0, Karlovitz numbers of 0-0.91 and unstretched laminar burning velocities of 130-1730 mm/s. It should be noted, however, that some entries are provisional as marked because they involved values of δ_D/r_f outside the allowable range and excessive effects of buoyancy.

Computational Methods

General Description

The numerical simulations of outwardly-propagating spherical flames were similar to past work for hydrogen/air flames.[4] The calculations were based on the unsteady, one-dimensional governing equations incorporated in the computer code RUN-1DL due to Rogg.[34] A second series of calculations for unstretched (plane) flames were carried out using the steady, one-dimensional laminar premixed flame computer code PREMIX due to Kee and coworkers.[35-39] In both cases thermochem-ical and transport properties were found from Kee et al.,[35-37] except for the thermochemical properties of HO_2 which were found from Kim et al.[6] All these properties were checked against original sources. Similar to the measurements, effects of radiation were ignored, and data were reduced from the simulation only where r_f was large enough so that

effects of initial conditions were negligible and $\delta_D/r_f \leq 0.02$ Several transport approximations were considered; the present calculations were carried out using the mixture-averaged multicomponent transport approximation plus thermal diffusion, but ignoring the Dufour effect, as justified in the Appendix. Other details concerning these calculations are reported in Ref. 4.

Chemical Reaction Mechanisms

Computations were limited to the chemical reaction mechanism for C/H/O kinetics due to Kim et al.[6] The potential importance of N/O chemistry was evaluated based on the mechanism of Miller and Bowman;[40] however, similar to earlier findings for hydrogen/air flames,[4] it was found that these reactions were not important for the flame properties of interest here so that N/O chemistry was ignored in order to minimize the complexity of the chemical reaction mechanism.

The final reduced chemical reaction mechanism (after eliminating N/O chemistry) due to Kim et al.[6] involved 12 species and 30 reversible reactions, not counting the range of third-body collision efficiencies considered. The backward rates were found from chemical equilibrium considerations using the CHEMKIN package.[37]

Results and Discussion

Flame Stability and Evolution

Three kinds of flame surface instabilities were observed during the present investigation: preferential-diffusion instability, hydrodynamic instability and buoyant instability. Preferential-diffusion instability (stability) is associated with negative (positive) Markstein numbers where bulges of the flame surface that are concave (convex) toward the combustion products have positive (negative) Karlovitz numbers (analogous to Eq. (5) for spherical flames) and thus increased (decreased) laminar burning velocities through Eq. (1); as a result, the bulges grow (decay) and the flame is unstable (stable) to preferential-diffusion effects. Hydrodynamic and buoyant instabilities were also observed; they are associated with accelerative effects of a light gas toward a heavy gas and gravity, respectively.

The typical appearance of the present flames at various stability conditions can be seen from the flame shadowgraphs appearing in Fig. 1. Four conditions are illustrated: stable/non-buoyant, where Ma = 7.6 yields rather stable conditions so that the flame surface is smooth; near-neutral/non-buoyant, where Ma = -0.8 so that marginal stability allows several crack-like disturbances from the ignition process and the ignition wires to persist throughout the period of flame propagation; stable/buoyant, where Ma = 7.3 is large enough to eliminate surface disturbances but the small laminar burning velocity allows buoyancy to distort the flame into an oblong shape; and unstable/nonbuoyant, where Ma = -6.5 yields numerous growing disturbances of the flame surface. The present unstable flames generally exhibited a much slower transition to the chaotically disturbed surface conditions observed in hydrogen/air flames;[1,4] instead, the disturbances seen for unstable conditions were similar to the early stages of hydrodynamic instability observed by Groff[41] and at larger radii for the present test configuration.[1-4] Thus, preferential diffusion instability for present conditions manifests itself as an inability to control hydrodynamic instabilities at relatively small flame radii, which generally agrees with the preferential diffusion instability growth mechanism described by Clavin.[7]

Typical of past work,[1-4] the onset of preferential diffusion instability was sufficiently delayed so that laminar burning velocities could be measured for a time before surface irregularities appeared to significantly modify the flame surface area. Similarly, the onset of hydrodynamic and/or buoyant instabilities was always observed at large radii so that these effects were not significant for the range of flame sizes considered here.

Typical measurements of laminar burning velocities as a function of flame radius are illustrated in Fig. 2 These results are for a hydrogen concentration of 50% by volume in the fuel mixture but results at other conditions were similar. Unstable preferential-diffusion conditions (Ma < 0) are denoted by darkened symbols while stable preferential-diffusion conditions are denoted by open symbols; this practice will be adopted on all subsequent plots. All these conditions involved relatively mild preferential-diffusion instabilities so that all measurements were carried out up to the r_f = 30 mm limit, even though some conditions are unstable. Nevertheless, classicial preferential-diffusion behavior can be seen with results for ϕ = 0.6, 0.8 and 1.2 exhibiting unstable behavior where S_L progressively decreases with increasing r_f (and thus decreasing Ka) while results for ϕ = 2.8, 4.0 and 4.5 exhibit stable behavior where S_L progressively increases with increasing r_f (and thus decreasing Ka). The fact that these changes persist until large radii, involve both

increases and decreases of S_L, and yield anticipated corresponding stability behavior as discussed in connection with Fig. 1, provides strong evidence that these variations of S_L are caused by preferential-diffusion phenomena.

Burning Velocity/Stretch Interactions

Similar to past results,[1-4] values of S_L as a function of Ka yielded linear plots according to Eq. (1), implying values of Ma that were independent of Ka over the present test range which could be extrapolated to Ka = 0 to estimate S_{L_o}. This procedure was used to find the values of S_{L_o} and Ma summarized in Table 1. Then given S_{L_o}, plots of S_{L_o}/S_L as a function of Ka can be constructed as suggested by Eq. (1). The same procedure was carried out for the numerically- simulated outwardly-propagating spherical flames, which also yielded values of S_{L_o}, Ma and plots of the results according to Eq. (1). Samples of these results are illustrated in Figs. 3 and 4 for low and high hydrogen concentrations, respectively. Thus Figs. 3a and b are measured and predicted values of S_{L_o}/S_L as a function of Ka for a hydrogen concentration of 10% by volume in the fuel mixture, while Figs. 4a and b are similar results for a hydrogen concentration of 50% in the fuel mixture. Results at other conditions over the present range of experiments are similar.

The results illustrated in Figs. 3 and 4 are similar to past findings for hydrogen and hydrocarbon-fueled flames at NTP.[1-4] Thus, the plots are linear yielding values of Ma independent of Ka and varying only with reactant mixture composition over the present test range. It should be recalled, however, that the present range of Ka is not close to extinction conditions (where Ka would be on the order of unity, see Law[3]) where the response of the flames to stretch is likely to differ. Even for the modest range illustrated, Ka < 0.25, however, effects of stretch are substantial with values of S_{L_o}/S_L varying in the range 0.6-2.2. Naturally, larger values of S_{L_o}/S_L are possible given larger values of Ka than those used during the present investigation. Thus, it is not surprising that effects of stretch on typical hydrogen and hydrocarbon-fueled flames are sufficient to modify the behavor of even very strongly turbulent flames.[1] Finally, the agreement between predictions and measurements is not as good for earlier results for hydrogen/air flames at NTP, with measurements tending to show greater degrees of unstable behavior than predicted. Comparisons between predictions and measurements are easier to quantify using Markstein numbers, however, which will be considered next.

Markstein Numbers

The measured values of Markstein numbers are summarized in Table 1, while both measurements and predictions over the entire test range are plotted in Fig. 5. For small concentrations of hydrogen in the fuel mixture, ≤ 5% by volume, present measurements of Ma ≈ 0 within experimental uncertainties (recall that results at the extreme values of fuel-equivalence ratios involve conditions outside planned tolerances for the present experiments and are somewhat suspect as a result). This behavior superfically agrees with qualitative ideas about preferential diffusion effects because the mass diffusivities of the major reactants (CO and O_2) and the diluent (N_2) are very similar. On the other hand, hydrogen is crucial for carbon-monoxide oxidation so that preferential diffusion of this fast-diffusing substance, and other light radicals, might be expected to cause greater sensitivity of these flames to stretch.

As hydrogen concentrations increase beyond 5% by volume in the fuel mixture, the results illustrated in Fig. 5 show that the sensitivity of the flames to stretch increases, e.g., absolute values of Ma increase. Uncertainties about the location of the neutral stability condition are relatively large because the range of fuel-equivalence ratios where Markstein numbers are small is relatively broad. Nevertheless, neutral conditions are observed near $\phi = 1$ when the hydrogen concentration in the fuel mixture is 50% by volume, which is not far from the neutral condition of $\phi = 0.7$ found for pure hydrogen/air flames at NTP.[4]

Comparisons between present values of Ma at large the hydrogen concentrations illustrated in Fig. 5 and results for pure hydrogen-fueled flames from Ref. 4 must be approached with caution because the values of D_u used to reduce the data differ. In particular, values of D_u have been selected for the major fuel component by convention;[1-4] thus, D_u = 20.2 mm²/s for carbon-monoxide in the present study and D_u = 72.9 mm²/s for hydrogen in Ref. 4. The effect of this difference in D_u on values of Ma and Ka can be seen by substituting δ_D from Eq. (3) into Eq. (2) to yield:

$$Ka = K D_u / S_L^2 , \quad Ma = L S_L / D_u \qquad (6)$$

It can be seen from Eq. (6) that present values of Ma for wet carbon-monoxide/air flames are numerically 3.6 times larger than those of Ref. 4 for hydrogen/air flames due to the different reference values of D_u used in the two studies. Thus, absolute values of Ma for hydrogen/air mixtures in Ref. 4 are significantly larger

than present results, even for hydrogen concentrations of 50% by volume in the fuel mixture, e.g., 2.80 times larger at a fuel-equivalence ratio of 4.5. This behavior is consistent with the generally weaker preferential diffusion effects observed in the present study compared to Ref. 4: flame surface distortions developed more slowly for unstable preferential diffusion conditions and similarly decayed more slowly for stable preferential diffusion conditions.

Predictions and measurements are in reasonably good qualitative agreement in Fig. 5, with predictions correctly indicating a relatively slow variation of Ma with ϕ at small hydrogen concentrations in the fuel, the tendency for unstable (stable) preferential diffusion behavior at fuel-lean (fuel-rich) conditions, and the tendency for absolute values of Markstein numbers to increase as the concentration of hydrogen in the fuel increases. The discrepancies between predictions and measurements, however, generally are larger for present wet carbon-monoxide/air flames than for the results of Ref. 4 for hydrogen/air flames. In part, this behavior is superficial because values of Ma are larger for the present results due to the different values of D_u used as just discussed. In addition, the chemical reaction mechanism used here involves more steps to consider C/O reactions than the H/O system alone, with corresponding increases in potential preferential diffusion effects, so that some reduction of the accuracy of predictions can be expected. Nevertheless, in view of the novelty of Markstein numbers as a property of laminar premixed flames, and the fact that development of chemical reaction mechanisms has not involved consideration of this property, there is an encouraging degree of agreement between measurements and predictions in Fig. 5.

Unstretched Laminar Burning Velocities

Values of laminar burning velocities from various sources are plotted as a function of fuel-equivalence ratio, with the concentration of hydrogen in the fuel mixture as a parameter, in Fig. 6. Results illustrated in the figure include the measurements of McLean et al.,[17] Vagelopoulos and Egolfopoulos,[21] Scholte and Vaags[22] and the present investigation, along with the predictions based on the kinetics of Kim et al.[6] from the present investigation. Except for the measurements of Scholte and Vaags,[22] all these results have been corrected to provide estimates of the unstretched laminar burning velocities of plane flames. The results of Scholte and Vaags[22] are in remarkably good agreement with the stretch-corrected results; nevertheless, this agreement is largely fortuitous as discussed by McLean et al.[17] The various stretch-corrected measurements are in reasonably good agreement with each other, except for fuel-rich conditions at larger hydrogen concentrations in the fuel mixture. These conditions also involve relatively large Markstein numbers, see Fig. 5, so that corrections for effects of stretch to find S_{L_u} probably contribute to these discrepancies.

Maximum values of stretch-corrected laminar burning velocities for wet carbon-monoxide/air flames generally were reached for fuel-equivalence ratios in the range 2.0-2.8, see Fig. 6 and Table 1. This behavior is in good agreement with earlier stretch-corrected results due to McLean et al.[17] Nevertheless, since maximum temperatures in these flames are achieved near the stoichiometric mixture ratio, modeling this behavior using simplified global one-step reaction concepts appears to be problematical.

The comparison between present predictions and measurements of unstretched laminar burning velocities in Fig. 6 is reasonably good, including estimation of fuel-equivalence ratios for maximum laminar burning velocities and effects of added hydrogen concentrations in the fuel mixture. This is particularly true for low concentrations of hydrogen in the fuel mixture, which is encouraging due to the importance of the C/O reactions that dominate these flames for practical hydrocarbon combustion processes. As a result, comments about the comparison between present predictions and measurements generally parallel the results of Ref. 4 for hydrogen/air flames. In particular, predictions are quite good at fuel-lean conditions, with somewhat larger discrepancies between predictions and measurements at fuel-rich conditions . Thus, the C/H/O reaction mechanism of Kim et al.[6] appears satisfactory for many purposes even though improvements at fuel-rich and hydrogen-rich conditions would be desirable.

Sensitivity Analysis

Insight about the most important chemical reactions needed to predict the laminar burning velocities of unstretched wet carbon-monoxide/air flames at NTP was sought by carrying out sensitivity calculations using the methods described by Kee et al.,[38] and Grcar et al.[39] The results using the Kim et al.[6] reaction mechanism are illustrated in Figs. 7 and 8 for concentrations of hydrogen in the fuel mixture of 3 and 50%, respectively, which bound present measurements. The findings pictured in these figures are normalized

sensitivities based on the unstretched mass burning rates at ϕ = 0.6, 0.8, 2.4, 3.0 and 5.0, which balances results about the maximum laminar burning velocity conditions. Results are presented in the figures for the eight reactions exhibiting the largest sensitivities over the present test range.

The reactions exhibiting the greatest sensitivities over the test range in Figs. 7 and 8 are $CO + OH = CO_2 + H$, $HO_2 + H = 2OH$, $HO_2 + H = H_2 + O_2$, $H + O_2 = O + OH$ and $H_2 + O = OH + H$. Kim et al.[6] attribute moderate uncertainty factors to all these reactions, in the range 1.5-2.0; therefore, they merit consideration in an effort to reduce the discrepancies between the predictions and measurements at fuel-rich conditions. In addition, recent studies of $CO + OH = CO_2 + H$ reaction have raised questions about past estimates of this reaction rate constant that merit consideration, see the discussion of McLean et al.[17] The remaining reactions only involve H/O chemistry and improvements that should be considered here are not very different from the discussion for hydrogen/air flames of Ref. 4.

Flame Structure/Stretch Interactions

The discrepancies between present predictions and measurements were modest; therefore, the predictions were used to provide some insight about effects of stretch on flame structure. This methodology involved numerical simulations of outwardly-propagating spherical flames for nearly-neutral, unstable and stable preferential- diffusion conditions. The effect of flame-structure/stretch interactions was found by comparing predicted results for moderate levels of stretch (Ka of 0.06 and 0.08) with corresponding predictions for unstretched (plane) flames.

The predicted structure of stretched and unstretched laminar premixed wet carbon-monoxide/air flames at NTP are illustrated in Figs. 9-11 for for near-neutral, unstable and stable preferential-diffusion conditions, respectively. Results illustrated in the figures include distributions of temperatures and species mole fractions as a function of distance through the flames. The origins of the length scales for both of unstretched and stretched flames in these figures are arbitrary and the latter do not represent the center of the outwardly-propagating spherical flames.

The effect of stretch on laminar burning velocities can be best seen from modifications of radical concentrations near the hot boundary of the flames. As a first example, consider the neutral conditions in Fig. 9 for ϕ = 0.6 and 3% H_2 by volume in the fuel mixture. In this case, temperature distributions and the maximum temperature are nearly the same for stretched and unstretched flames, which yields nearly identical distributions of radicals. As a result, it is not very surprising that laminar burning velocities for the two conditions are nearly the same and $Ma \approx 0$.

The response of flame structure to stretch for unstable flames is illustrated in Fig. 10 for ϕ = 0.6 and 50% H_2 by volume in the fuel mixture. In this case, finite levels of stretch cause flame temperatures to be higher for the stretched flame (roughly 1900 K) than the unstretched flame (roughly 1800 K). This behavior is mainly caused by preferential diffusion where the faster diffusion of hydrogen compared to oxygen causes the flame to become more nearly stoichiometric (note the relatively larger concentrations of water vapor compared to carbon dioxide for the stretched flame in Fig. 10). This causes radical concentrations in the reaction zone of the stretched flame to increase compared to the unstretched flame (for example, the maximum mole fraction of OH is roughly 0.0063 in the stretched flame but only 0.0053 in the unstretched flame) promoting faster reaction rates and thus larger laminar burning velocities in the stretched flame.

The response of flame structure to stretch for stable flames is illustrated in Fig. 11 for ϕ = 4.0 and 50% H_2 by volume in the fuel mixture. In this case, finite levels of stretch cause flame temperatures to be lower for the stretched flame (roughly 1500 K) than for the unstretched flame (roughly 1550 K). This behavior also is due to effects of preferential diffusion, where the faster diffusion of hydrogen compared to oxygen causes the flame to become richer, decreasing the flame temperature when the flame is stretched. This causes radical concentrations in the reaction zone of the stretched flame to decrease compared to the stretched flame (for example, the maximum mole fraction of H is roughly 0.020 in the stretched flame compared to roughly 0.023 in the unstretched flame) promoting slower reaction rates and thus smaller laminar burning velocities for the stretched flame.

Effects of stretch on flame structure, and thus laminar burning velocities, are more complex at intermediate conditions than at the limiting conditions illustrated in Figs. 9-11. In the intermediate regime, effects of preferential diffusion of heat and mass and the propensity for added hydrogen to increase radical concentrations by dissociation to H even though flame temperatures are decreasing, become factors similar to the behavior of hydrogen/air flames discussed in Ref. 4.

Conclusions

Effects of positive stretch on the laminar burning velocities and structure of wet carbon-monoxide/air flames at NTP were studied experimentally and computationally. The measurements involved outwardly-propagating spherical flames using methods developed earlier,[1-4] while computations involved numerical simulations of the same flames using the chemical reaction mechanism of Kim et al.[6] Test conditions included concentrations of hydrogen in the fuel mixture of 3-50% by volume, fuel-equivalence ratios of 0.6-5.0, Karlovitz numbers of 0-0.9 and unstretched laminar burning velocities of 130-1730 mm/s. The major conclusions of the study are as follows:

1. Preferential-diffusion/stretch interactions correlated reasonably well using the local-conditions hypothesis similar to past work,[1-4] yielding Markstein numbers that were relatively independent of Karlovitz numbers for present test conditions.

2. Effects of preferential-diffusion/stretch interactions were substantial, yielding Markstein numbers of -6.5 to 7.6, with corresponding variations of $S_{L,u}/S_L$ of 0.6-2.3, reaching largest values near limits for large hydrogen concentrations.

3. Present measurements of unstretched laminar burning velocities were in good agreement with earlier stretch-corrected measurements of McLean et al.[17] and Vagelopoulos and Egolfopoulos,[21] with greatest discrepancies observed where Markstein numbers, and thus preferential- diffusion/stretch interactions, were large.

4. Predicted and measured unstretched laminar burning velocities and Markstein numbers were in fair agreement, using the reaction mechanism of Kim et al.,[6] but additional development of the mechanism is needed to improve predictions of Markstein numbers over the test range and unstretched laminar burning velocities for fuel-rich conditions at large hydrogen concentrations.

5. Effects of preferential-diffusion instabilities were properly observed at negative Markstein numbers and caused progressive growth of disturbances of the flame surfaces typical of hydrodynamic instabilities relatively early in the flame propagation process; nevertheless, disturbances of the flame surfaces typical of hydrodynamic instabilities were still observed at large flame radii even when Markstein numbers were positive.

Acknowledgements

This research was supported by NSF Grant Nos. CTS-9019813 and 9321959 under the technical management of M. J. Linevsky. Support from the Peace Fellowship Program of Egypt for one of us (M. I. Hassan) and useful discussions with B. Rogg are also gratefully acknowledged. L.-K. Tseng assisted with the initial phases of the research.

References

[1]Kwon, S., Tseng, L.-K. and Faeth, G.M., "Laminar Burning Velocities and Transition to Unstable Flames in $H_2/O_2/N_2$ and $C_3H_8/O_2/N_2$ Mixtures," Combust. Flame, Vol. 90, 1992, pp.230-246.

[2]Tseng, L.-K., Ismail, M.A. and Faeth, G.M., "Laminar Burning Velocities and Markstein Numbers of Hydrocarbon/Air Flames," Combust. Flame, Vol. 95, 1993, pp. 410-426.

[3]Aung, K.T., Tseng, L.-K., Ismail, M.A. and Faeth, G.M., "Response to Comment by S.C. Taylor and D.B. Smith on "Laminar Burning Velocities and Markstein Numbers of Hydrocarbon/Air Flames," Combust. Flame, Vol. 102, 1995, pp. 526-530.

[4]Aung, K.T., Hassan, M.I. and Faeth, G.M., "Flame/Stretch Interactions of Laminar Premixed Hydrogen/Air Flames at Normal Temperature and Pressure," Combust. Flame, submitted

[5]Yetter, R.A., Dryer, F.L. and Rabitz, H. "A Comprehensive Reaction Mechanism for Carbon Monoxide/Hydrogen/Oxygen Kinetics," Combust. Sci. Tech., Vol. 79, 1991, pp. 97-128.

[6]Kim, T.J., Yetter, R.A. and Dryer, F.L., "New Results on Moist CO Oxidation: High Pressure, High Temperature Experiments and Comprehensive Modeling," *Twenty-Fifth Symposium (International) on Combustion*, The Combustion Institute, Pittsburgh, 1994, pp. 759-766.

[7]Clavin, P., "Dynamic Behavior of Premixed Flame Fronts in Laminar and Turbulent Flows," Prog. Energy Combust. Sci., Vol. 11, 1985, pp. 1-59.

[8]Peters, N., "Laminar Flamelet Concepts in Turbulent Combustion," *Twenty-First Symposium (International) on Combustion*, The Combustion Institute, Pittsburgh, 1986, pp. 1231-1250.

[9]Law, C.K., "Dynamics of Stretched Flames," *Twenty-Second Symposium (International) on Combustion*, The Combustion Institute, Pittsburgh, 1988, pp. 1381-1402.

[10]Dixon-Lewis, G., "Structure of Laminar Flames," *Twentieth Symposium (International) on Combustion*, The Combustion Institute, Pittsburgh, 1990, pp. 305-324.

[11]Egolfopoulos, F.N. and Law, C.K., "An Experimental and Computational Study of the Burning Rates of Ultra-Lean to Moderately-Rich $H_2/O_2/N_2$ Laminar Flames with Pressure Variations," *Twenty-Third Symposium (International) on Combustion*, The Combustion Institute, Pittsburgh, 1990, pp. 333-340.

[12]Law, C.K., "A Compilation of Experimental Data on Laminar Burning Velocities," *Reduced Kinetic Mechanisms for Applications in Combustion Systems* (N. Peters and B. Rogg, eds.), Springer-Verlag, Berlin, 1993, pp. 15-26.

[13]Searby, G. and Quinard, J., "Direct and Indirect Measurements of Markstein Numbers of Premixed Flames," Combust. Flame, Vol. 82, 1990, pp. 298-311.

[14]Deshaies, B. and Cambray, P., "The Velocity of a Premixed Flame as a Function of the Flame Stretch: An Experimental Study," Combust. Flame, Vol. 82, 1990, pp. 361-375.

[15]Dowdy, D.R., Smith, D.B., Taylor, S.C. and Williams, A., "The Use of Expanding Spherical Flames to Determine Burning Velocities and Stretch Effects on Hydrogen/Air Mixtures," *Twenty-Third Symposium (International) on Combustion*, The Combustion Institute, Pittsburgh, 1990, pp. 325-333.

[16]Taylor, S.C., "Burning Velocity and Influence of Flame Stretch," Ph.D. Thesis, University of Leeds, 1991.

[17]McLean, I.C., Smith, D.B. and Taylor, S.C., "The Use of Carbon Monoxide/Hydrogen Burning Velocities to Examine the Rate of the CO + OH Reaction," *Twenty-Fifth Symposium (International) on Combustion*, The Combustion Institute, Pittsburgh, 1994, pp. 749-757.

[18]Mishra, D.P., Paul, P.J. and Mukunda, H.S., "Stretch Effects Extracted from Propagating Spherical Premixed Flames with Detailed Chemistry," Combust. Flame, Vol. 99, 1994, pp. 379-386.

[19]Mishra, D.P., Paul, P.J. and Mukunda, H.S., "Stretch Effects Extracted from Inwardly and Outwardly Propagating Spherical Premixed Flames," Combust. Flame, Vol. 97, 1994, pp. 35-47.

[20]Markstein, G.H., *Non-Steady Flame Propagation*, Pergamon, New York, 1991, p. 22.

[21]Vagelopoulos, C.M. and Egolfopoulos, F.N., "Laminar Flame Speeds and Extinction Strain Rates of Mixtures of Carbon Monoxide with Hydrogen, Methane, and Air," *Twenty-Fifth Symposium (International) on Combustion*, The Combustion Institute, Pittsburgh, 1994, pp. 1317-1328.

[22]Scholte, T.G. and Vaags, P.B., "Burning Velocity of Mixtures of Hydrogen, Carbon Monoxide and Methane with Air," Combust. Flame, Vol. 3, 1959, pp. 511-524.

[23]Jahn, G., cited in Lewis, B. and von Elbe, G.,*Combustion Flames and Explosions of Gases*, 3rd ed., Academic Press, New York, 1987, pp. 395-402.

[24]Gunther, R. and Janisch, G., "Messwerte der Flammegeschwindigkeit von Gasen und Gasgemischen," Chemie-Ing.-Techn., Vol. 43, 1971, p. 975.

[25]Gunther, R. and Janisch, G., "Measurement of Burning Velocity in a Flat Flame Front," Combust. Flame, Vol. 19, 1972, pp. 49-53.

[26]Yumlu, V.S., "Prediction of Burning Velocities of Carbon Monoxide-Hydrogen-Air Flames," Combust. Flame, Vol. 11, 1967, pp. 190-194.

[27]Strauss, W.A. and Edse, R., "Burning Velocity Measurements by the Constant-Pressure Bomb Method," *Seventh Symposium (International) on Combustion*, The Combustion Institute, Pittsburgh, 1958, pp. 377-385.

[28]Cherian, M.A., Rhodes, P., Simpson, R.J. and Dixon-Lewis, G., "Kinetic Modelling of the Oxidation

of Carbon Monoxide in Flames," *Eighteenth Symposium (International) on Combustion*, The Combustion Institute, Pittsburgh, 1981, pp. 385-396.

[29]Olsson, J.O. and Olsson, I.B.M., "Detailed Computer Modeling on a Premixed Laminar Carbon Monoxide/Hydrogen Flame," J. Phys. Chem., Vol. 96, 1992, pp. 690-696.

[30]Siegel, R. and Howell, J.R., *Thermal Radiation Heat Transfer*, 2nd ed., McGraw-Hill, New York, 1981, pp. 613-627.

[31]Strehlow, R.A. and Savage, L.D., "The Concept of Flame Stretch," Combust. Flame, Vol. 31, 1978, pp. 209-211.

[32]Gordon, S. and McBride, B. J., "Computer Program for Calculation of Complex Chemical Equilibrium Compositions, Rocket Performance, Incident and Reflected Shocks, and Chapman-Jouguet Detonations," NASA SP-273, 1971.

[33]Lewis, B. and von Elbe, G., *Combustion, Flames and Explosions of Gases*, 2nd ed., Academic Press, New York, 1961, pp. 381-384.

[34]Rogg, B. "RUN-1DL: The Cambridge Universal Laminar Flame Code," Technical Report CUED/A-THERMO/TR39, Depart-ment of Engineering, University of Cambridge, 1991.

[35]Kee, R.J., Dixon-Lewis, G., Warnatz, J., Coltrin, M.E. and Miller, J.A., "A FORTRAN Computer Code Package for the Evaluation of Gas-Phase, Multicomponent Transport Properties," Sandia National Laboratories, Report SAND86-8246, 1986.

[36]Kee, R.J., Ripley, F.M. and Miller, J.A., "The CHEMKIN Thermodynamic Data Base," Sandia National Laboratories, Report No. SAND87-8215B, 1990.

[37]Kee, R.J., Ripley, F.M. and Miller, J.A., "CHEMKIN II: A Fortran Chemical Kinetics Package for the Analysis of Gas Phase Chemical Kinetics," Sandia National Laboratories, Report No. SAND89-8009B, 1991.

[38]Kee, R.J., Grcar, J.F., Smooke, M.D. and Miller, J.A., "A Fortran Program for Modeling Steady Laminar One-Dimensional Premixed Flames," Sandia National Laboratories, Report No. SAND85-8240, 1993.

[39]Grcar, J.F., Kee, R.J., Smooke, M.D. and Miller, J.A., "A Hybrid Newton/Time-Integration Procedure for the Solution of Steady, Laminar, One-Dimensional, Premixed Flames," *Twenty-First Symposium (International) on Combustion*, The Combustion Institute, Pittsburgh, 1986, pp. 1773-1782.

[40]Miller, J.A. and Bowman, C.T., "Mechanism and Modeling of Nitrogen Chemistry in Combustion," Prog. Energy Combust. Sci., Vol. 15, 1989, pp. 287-338.

[41]Groff, E.G., "The Cellular Nature of Confined Spherical Propane-Air Flames," Combust. Flame, Vol. 48, 1982, pp. 51-62.

Appendix:
Evaluation of Transport Approximations

The effect of transport model approximations on the predictions of $S_{L,-}$ as a function of ϕ for wet carbon-monoxide/air flames at NTP did not vary significantly with H_2 concentration. Thus, typical behavior is illustrated in Fig. 12 for a concentration of hydrogen in the fuel mixture of 3% by volume. Four sets of calculations are illustrated, involving progressively more complete treatments of transport, as follows: mixture-averaged multicomponent mass diffusion (MIX), mixture-averaged multicomponent mass diffusion plus thermal diffusion (MIX-TDIF), complete multicomponent mass diffusion (MULT) and complete multicomponent mass diffusion plus thermal diffusion (MULT-TDIF). Computations for complete multicomponent mass diffusion plus both thermal diffusion and the Duflour effect were considered as well but these results were identical to the MULT-TDIF results, similar to earlier work,[4] and were not considered any further. The predictions illustrated in Fig. 12 indicate significant effects of thermal diffusion but with differences between MULT-TDIF and MIX-TDIF generally less than 10% for the present range of flame conditions. These latter differences are comparable to present experimental uncertainties; therefore, present calculations were carried out using the MIX-TDIF approach in order to control computer costs, similar to earlier work.[4]

Table 1 Summary of Test Conditions[a]

ϕ	0.6	0.8	1.0	1.2	1.6	2.0	2.4	2.8	3.0	3.5	4.0	4.5	5.0
97%CO+3%H2													
ρ_u/ρ_b	5.94	6.67	6.98	7.06	6.83	6.45	6.10		5.65	5.33	5.06		4.60
$S_{L,o}$ (mm/s)	130[b]	220	260	330	430	470	470		460	440	320		200[c]
Ka_{max}	0.91	0.27	0.18	0.13	0.19	0.14	0.13		0.11	0.14	0.21		0.30
Ma	1.4	0.8	-0.2	-1.2	-1.0	-0.5	-0.2		-0.3	0.1	-0.1		1.8
95%CO+5%H2													
ρ_u/ρ_b	5.82	6.66	6.98	7.06	6.82	6.43	6.08	5.78	5.63	5.32	5.04	4.80	4.59
$S_{L,o}$ (mm/s)	200[b]	280	340	430	520	590	630	630	590	580	480	400	280[c]
Ka_{max}	0.17	0.14	0.13	0.14	0.10	0.09	0.09	0.09	0.10	0.08	0.08	0.08	0.14
Ma	-1.2	-0.4	-0.9	0.3	-0.1	-0.2	1.1	0.7	0.1	0.0	0.9	0.1	1.6
90%CO+10%H2													
ρ_u/ρ_b	5.79	6.65	6.97	7.04	6.79	6.40	6.05	5.74	5.60	5.29	5.02	4.78	4.57
$S_{L,o}$ (mm/s)	240	360	550	540	710	790	830	790	790	730	540	410	290[c]
Ka_{max}	0.17	0.18	0.12	0.11	0.10	0.07	0.06	0.07	0.06	0.08	0.09	0.08	0.12
Ma	-1.1	-0.5	-0.5	0.4	0.6	0.9	1.1	2.1	2.5	1.3	2.5	2.2	2.2
75%CO+25%H2													
ρ_u/ρ_b	5.86	6.61	6.95	7.01	6.71	6.31	5.97	5.66	5.53	5.22	4.95	4.71	4.51
$S_{L,o}$ (mm/s)	320	520	710	830	1070	1160	1160	1110	1030	840	640	410	290[c]
Ka_{max}	0.09	0.09	0.08	0.08	0.07	0.06	0.06	0.04	0.05	0.06	0.06	0.18	0.28
Ma	-3.3	-2.3	-1.4	-0.8	0.9	0.8	0.2	0.4	2.4	3.5	3.5	4.3	7.3
50%CO+50%H2													
ρ_u/ρ_b	5.76	6.55	7.01	6.96	6.60	6.21	5.87	5.58	5.44	5.14	4.87	4.65	
$S_{L,o}$ (mm/s)	500	880	1100	1290	1650	1730	1700	1520	1370	1070	880	560	
Ka_{max}	0.07	0.07	0.06	0.05	0.04	0.04	0.04	0.03	0.05	0.06	0.08	0.14	
Ma	-6.5	-3.4	-2.4	-0.9	0.3	1.4	0.9	3.0	2.9	4.4	4.4	7.6	

[a] CO/H2/air flames at NTP condition, (D_u=20.2 mm²/s).
[b] Provisional results because δ_D/r_f >0.02 for a portion of the data base.
[c] Provisional results because the flame was somewhat distorted by buoyancy for a portion of the data base.

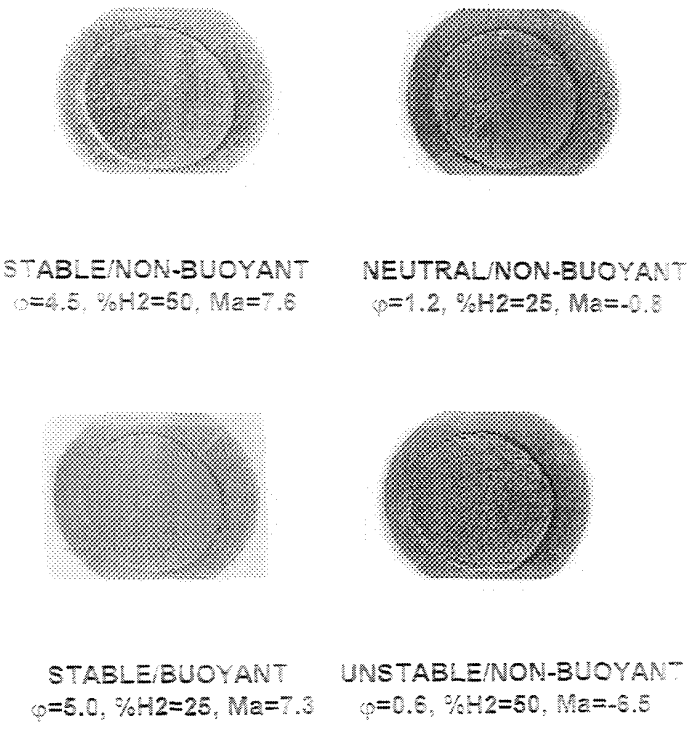

Fig. 1 Photographs of flames for various stability conditions.

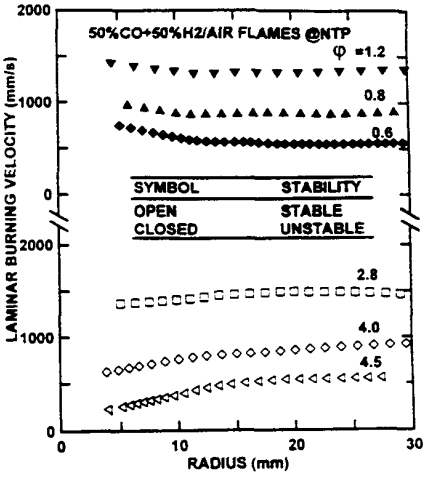

Fig. 2 Typical plots of laminar burning velocities as a function of flame radius for H_2 concentrations in the fuel of 50% by volume.

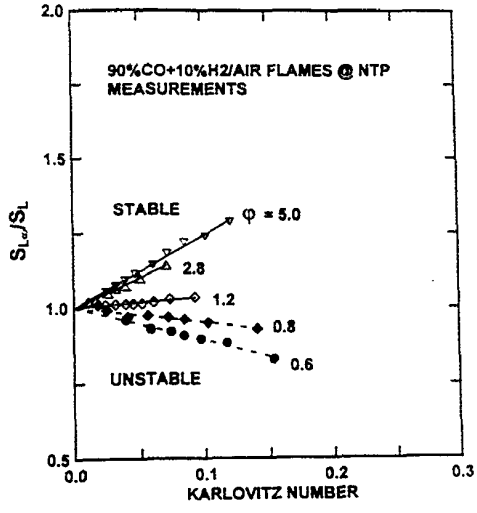

Fig. 3a Measured laminar burning velocities as a function of Karlovitz numbers and fuel-equivalence ratios for H_2 concentrations in the fuel of 10% by volume.

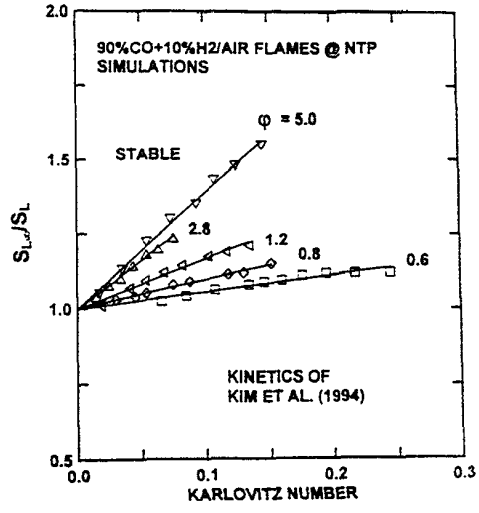

Fig. 3b Predicted laminar burning velocities as a function of Karlovitz numbers and fuel-equivalence ratios for H_2 concentrations in the fuel of 10% by volume.

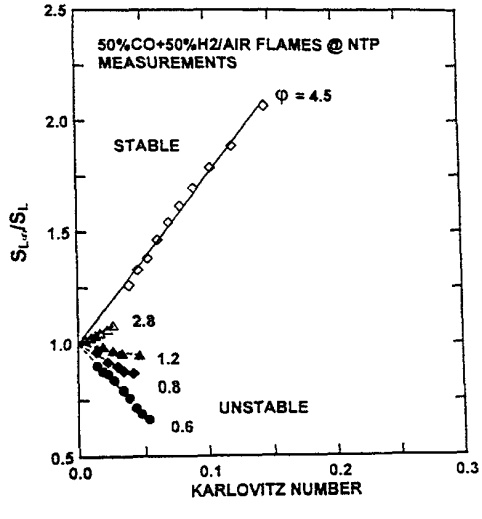

Fig. 4a Measured laminar burning velocities as a function of Karlovitz numbers and fuel-equivalence ratios for H_2 concentrations in the fuel of 50% by volume.

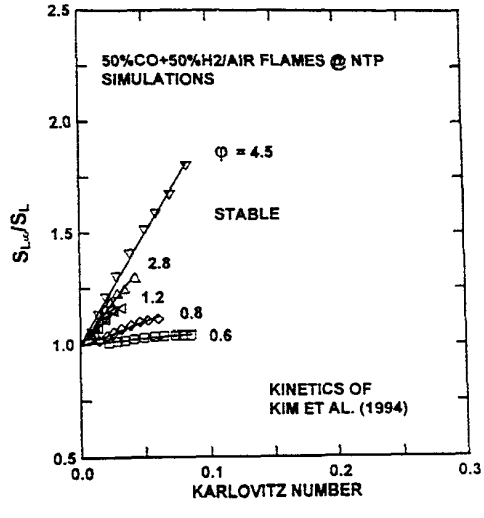

Fig. 4b Predicted laminar burning velocities as a function of Karlovitz numbers and fuel-equivalence ratios for H_2 concentrations in the fuel of 50% by volume.

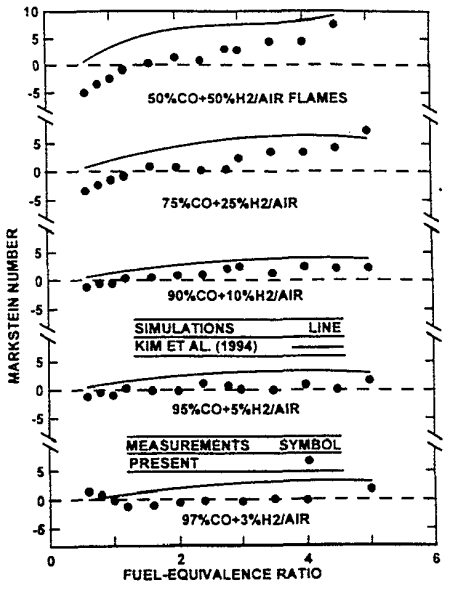

Fig. 5 Measured and predicted Markstein numbers as a function of fuel-equivalence ratios and hydrogen concentrations in the fuel.

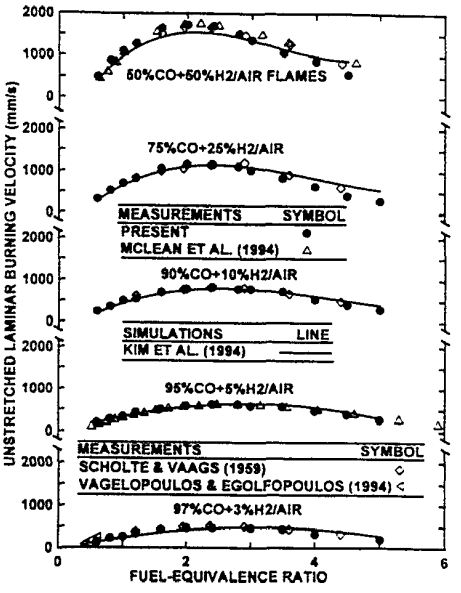

Fig. 6 Measured and predicted laminar burning velocities as a function of fuel-equivalence ratios and hydrogen concentrations in the fuel.

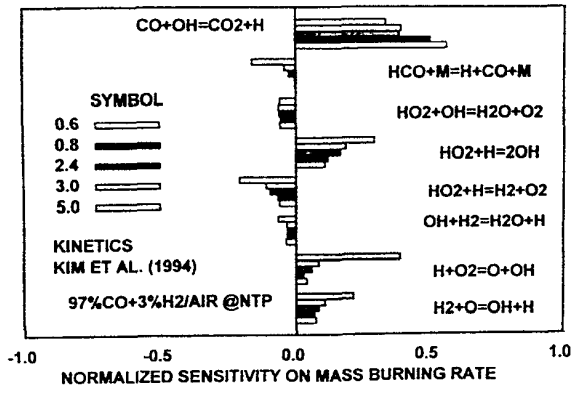

Fig. 7 Normalized sensitivities of kinetic parameters for unstretched laminar burning velocities at various fuel-equivalence ratios for H_2 concentrations in the fuel of 3% by volume.

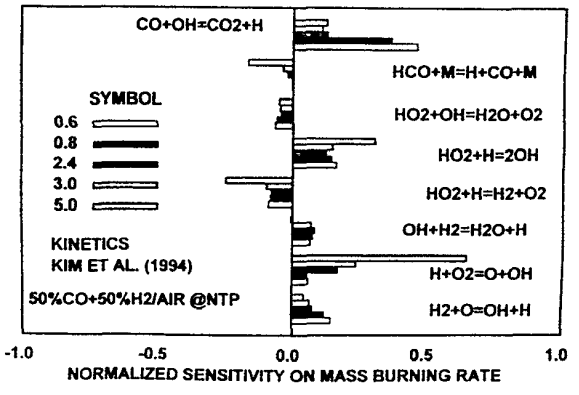

Fig. 8 Normalized sensitivities of kinetic parameters for unstretched laminar burning velocities at various fuel-equivalence ratios for H_2 concentrations in the fuel of 50% by volume.

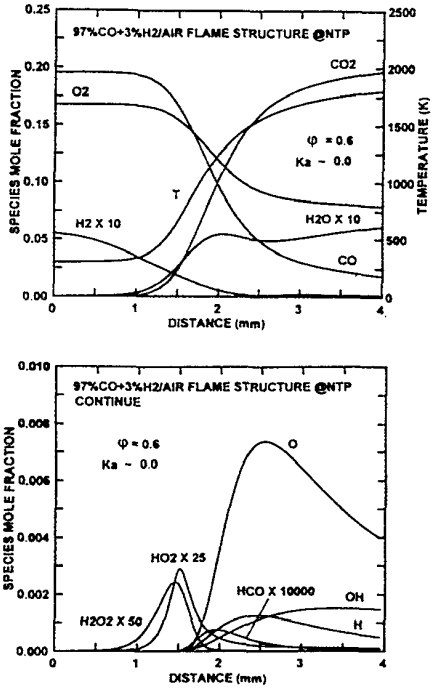

Fig. 9a Predicted structure of an unstretched flame for near-neutral preferential-diffusion conditions (3% H_2 and $\phi = 0.6$).

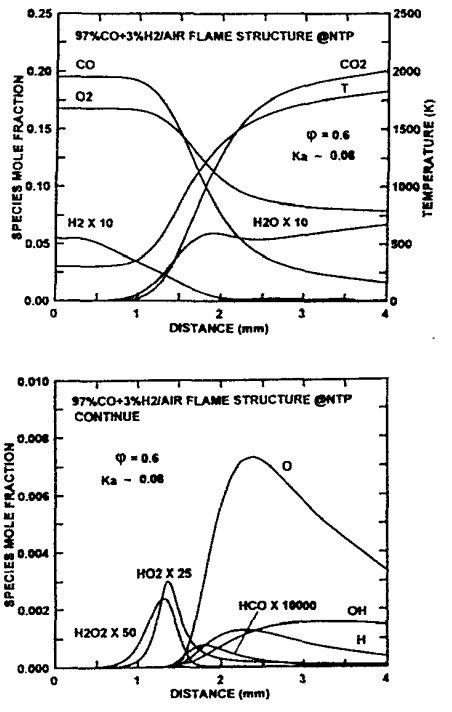

Fig. 9b Predicted structure of a stretched flame (Ka ~ 0.08) for near-neutral preferential-diffusion conditions (3% H_2 and $\phi = 0.6$).

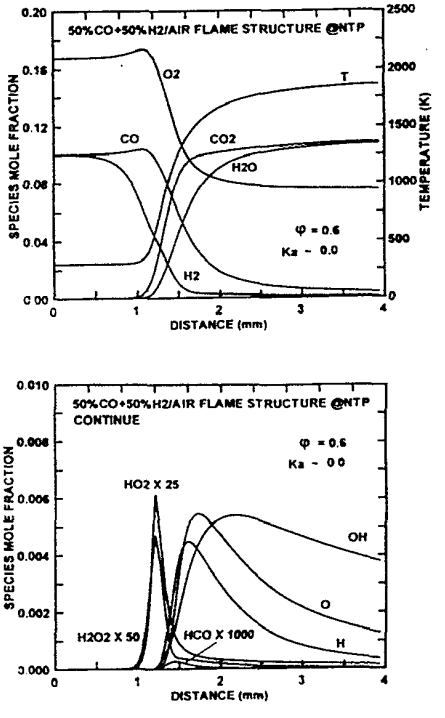

Fig. 10a Predicted structure of an unstretched flame for unstable preferential-diffusion conditions (50% H_2 and $\phi = 0.6$).

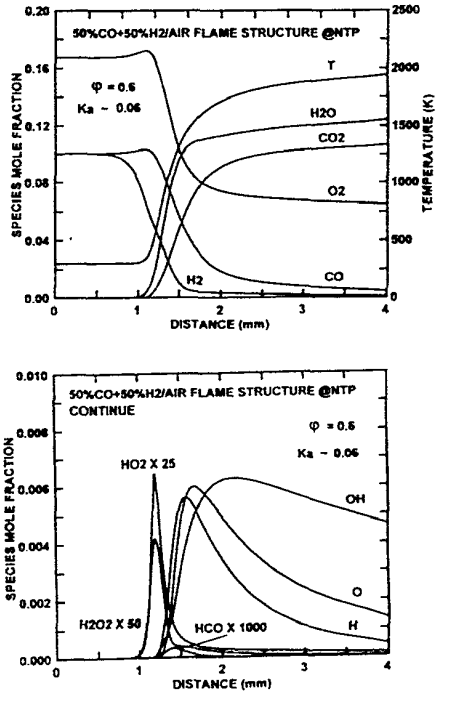

Fig. 10b Predicted structure of a stretched flame (Ka ~ 0.06) for unstable preferential-diffusion conditions (50% H_2 and $\phi = 0.6$).

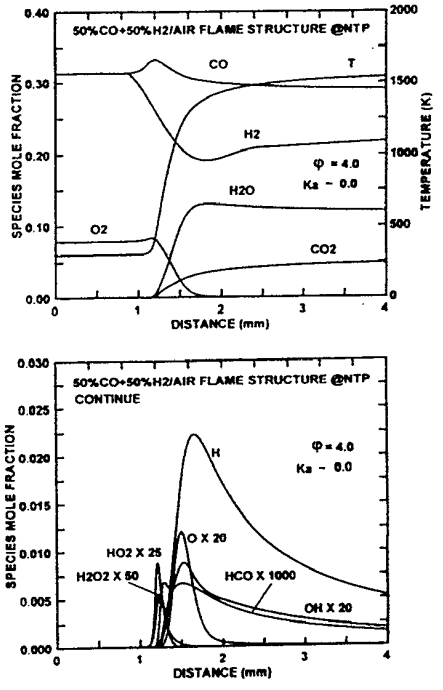

Fig. 11a Predicted structure of an unstretched flame for unstable preferential diffusion conditions (50% H_2 and $\phi = 4.0$).

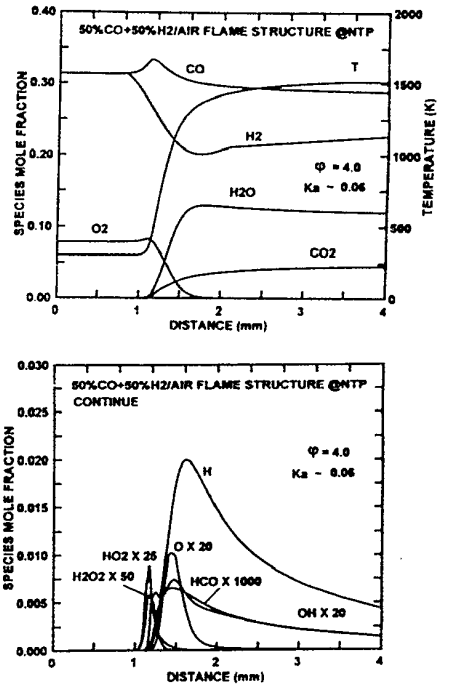

Fig. 11b Predicted structure of a stretched flame (Ka ~ 0.06) for stable preferential-diffusion conditions (50% H_2 and $\phi = 4.0$).

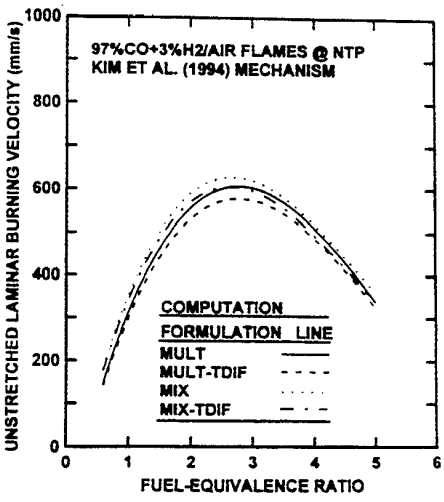

Fig. 12 Effect of transport model approximations on unstretched laminar burning velocity predictions for 3% H_2 flames.